Available online at www.sciencedirect.com
SCIENCE DIRECT
Sedimentary Geology 180 (2005) 149–166
Sedimentary Geology
www.elsevier.com/locate/sedgeo

Late-Holocene evolution of the Mahakam delta, East Kalimantan, Indonesia

Joep E.A. Storms [a,*], Robert M. Hoogendoorn [a], Rien A.C. Dam [a], A.J.F. Hoitink [b,c], S.B. Kroonenberg [a]

[a] *Delft University of Technology, Faculty of Civil Engineering and Geosciences, Department of Geotechnology, Section of Applied Geology, Mijnbouwstraat 120, 2628 RX, Delft, The Netherlands*

[b] *Wageningen University, Department of Environmental Sciences, Hydrology and Quantitative Water Management Group, Nieuwe Kanaal 11, 6709 PA Wageningen, The Netherlands*

[c] *Utrecht University, Department of Physical Geography, Institute for Marine and Atmospheric Research, P.O. Box 80.115, 3508 TC Utrecht, The Netherlands*

Received 16 December 2004; received in revised form 17 August 2005; accepted 22 August 2005

Abstract

The late-Holocene Mahakam delta, located along the tropical eastern shore of Kalimantan, Indonesia, is considered to be a textbook example of a mixed tide–fluvial dominated delta system. The delta prograded about 60 km during the past 5000 years, which led to the development of a distinct network of distributary and tidal channels. Wave action is low due the limited fetch in the narrow strait of Makassar. Mahakam River discharge is about a quarter of the Mississippi River discharge and is characterized by absence of flood surges. Therefore, natural levees, crevasse splays and avulsions are absent in the delta plain. For the past four decennia, both modern and ancient Mahakam delta deposits have been studied in detail in order to better understand subsurface Miocene and Tertiary Mahakam deposits, which host large volumes of hydrocarbons.

This study focuses on the dynamics and stratal patterns of delta plain, delta-front platform deposits and suspended sediments. Due to the predominance of semi-diurnal tides and the associated flow reversals, depositional patterns are highly variable which has resulted in the formation of characteristic sand–mud couplets. The distribution of the sand–mud couplets found in this study differs from previously proposed conceptual models. They are limited to the fluvial domain and form in the distributary channels (lateral channel bar) or at the fluvial dominated delta-front platform, which flanks the mouth bar deposits in offshore direction. The sand–mud couplets which formed as delta-front platform and lateral channel bar deposits are similar and can only be identified based on their ^{14}C age. The sand content decreases significantly towards the tidal dominated areas due to limitation in transport capacity. Turbidity measurements taken in front of the river mouth also show rapid settlement of river plume sediments.

Some 22 new AMS ^{14}C dates show that late Holocene sea level history resembles the eustatic sea level curve giving a first approximation of the Late Holocene sea level history for East Kalimantan. The dates suggest that the progradational delta system evolved under conditions of slowly rising sea level, which compares well to the eustatic sea level curve. In addition, calculated

* Corresponding author. Present address: Delft University of Technology, Faculty of Civil Engineering and Geosciences, Department of Civil Engineering, section of Hydraulic Engineering, Stevinweg 1, 2628 CN Delft, The Netherlands.
E-mail address: j.e.a.storms@citg.tudelft.nl (J.E.A. Storms).

0037-0738/$ - see front matter © 2005 Elsevier B.V. All rights reserved.
doi:10.1016/j.sedgeo.2005.08.003

averaged deposition rates of the sand–mud couplets indicate that deposition is driven by the spring–neap tide cycles instead of the daily tidal cycle.
© 2005 Elsevier B.V. All rights reserved.

Keywords: Tidalites; Sea level; Radiocarbon dates; Subaqueous delta; Fluvial processes; Distributary channels

1. Introduction

The late-Holocene Mahakam delta, located along the tropical eastern shore of Kalimantan, Indonesia (Fig. 1) prograded about 60 km during the past 5000 years which led to the development of a distinct network of distributary and tidal channels, that has formed a lobate, fan shaped delta. The present day subaerial delta covers ~1800 km^2 of partly undeveloped tropical lowland forest, *Nypa* swamps and a mangrove shoreline (Fig. 2). Based on the morphologic characteristics, the Mahakam delta is considered to be a textbook example of a mixed tide–fluvial dominated delta system (Galloway, 1975). Yet, only few studies have examined the interaction between tidal and fluvial processes at the Mahakam delta, in contrast to other fluvial-tide dominated systems, for example the Ganges–Brahmaputra (Goodbred and Kuehl, 1999), McArthur river (Jones et al., 2003) and the Seine (Lesueur et al., 2003). The origin and distribution of fluvial deltaic facies in relation to tidal processes remains controversial for the Mahakam delta, despite detailed studies of both modern and ancient Mahakam sediments (Allen and Chambers, 1998; Allen et al., 1977; Allen and Mercier, 1994; Gastaldo et al., 1995; Gastaldo and Huc, 1992). The main focus of these studies has been the modern mouth bar, channel and delta-front slope that share many similarities with the Miocene and Tertiary Mahakam delta deposits, which host large volumes of hydrocarbons (Howes, 1997).

The pioneering work by Allen et al. (1977) on the evolution of the modern Mahakam is still a standard reference work describing the individual depositional environments that comprise the delta plain, delta-front platform, delta-front slope and prodelta environments (Fig. 2). A deep core (MISEDOR; 638 m) was drilled in 1984 by IFREMER in the southern part of the modern Mahakam delta (Caratini and Tissot, 1988). Based on this core, Pleistocene and Holocene Mahakam facies are described using palynological studies. Four radiocarbon dates establish the depths of the Pleistocene base over which the early Holocene transgressive sequence and the late Holocene prograding sequence were deposited (Caratini and Tissot, 1988; Carbonel and Moyes, 1987). In the 1990s, the focus of research shifted to the Pleistocene and Holocene offshore deposits as high-resolution shallow seismic data became available (Roberts and Sydow, 1996, 2003; Snedden et al., 1996; Suiter, 1996). They reconstructed the delta development back to the Late Pleistocene in detail.

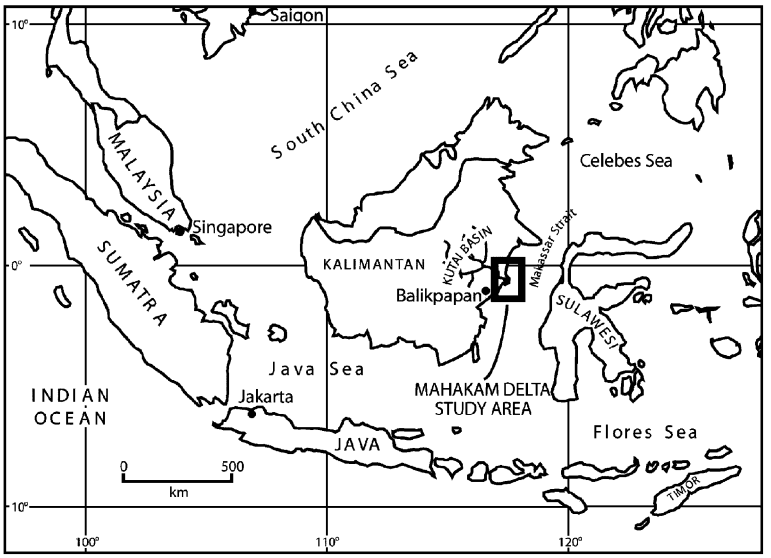

Fig. 1. Location map for the Mahakam delta study area on the east coast of Kalimantan, Indonesia (after Roberts and Sydow, 2003).

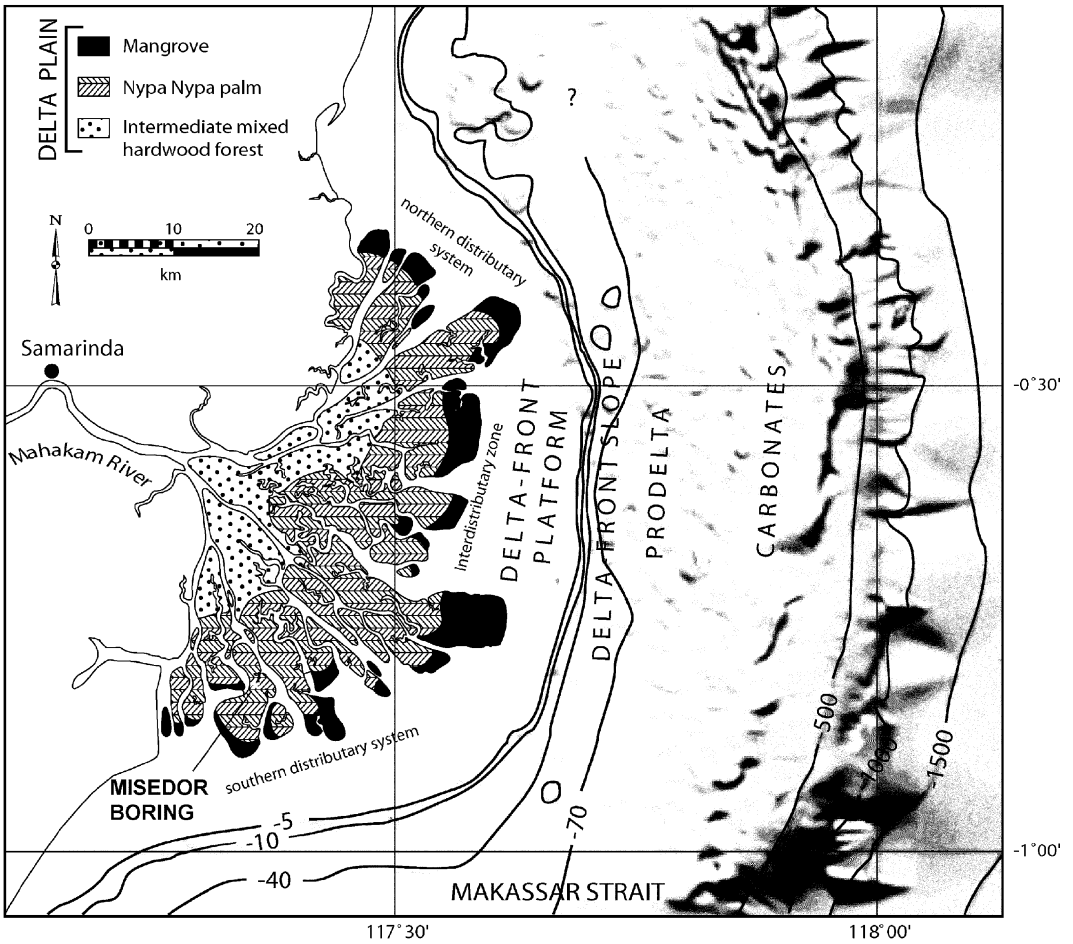

Fig. 2. Map of the study area showing the subaerial Mahakam delta plain with vegetation zones (after Allen and Chambers, 1998) and a shaded relief presentation of shelf and slope bathymetry (after Roberts and Sydow, 2003). Contours are in metres.

Until then, very little was known about the delta-front slope and prodelta deposits of both the modern as well as the Pleistocene Mahakam depositional units. However, as no seismic and core data were retrieved beyond the sub-tidal zone, the extent of the distribution of deltaic facies in relation to tidal processes and fluvial dynamics remained unexplored.

Following the early work of Allen et al. (1977) this paper focuses on understanding the interaction between tidal and fluvial processes that led to the formation of the late-Holocene delta plain and delta-front platform morphology and stratigraphy. Onshore shallow cores, suspended sediment measurements and new AMS ^{14}C dates provide new insight in the spatial distribution of delta plain and delta-front platform deposits. We propose a depositional mechanism that explains the cross- and along-shore heterogeneity found in the delta plain and delta-front platform deposits. In addition, the AMS ^{14}C dates give insights into spatial deposition rates and provide a first indication of the local sea level history.

2. Regional setting

2.1. Geologic setting

The modern Mahakam delta is located in the lower part of the Kutei Basin, which is situated on the east coast of Kalimantan, Indonesia, just south of the equator. The Kutei basin was initiated by rifting during the middle Eocene and was subsequently filled by syn-rift clastic sedimentation as well as carbonates until the early Miocene (Payenberg et al., 2003). The complete section up to the lower Miocene was subsequently folded to form the Samarinda anticlinorium, which became the basement for continuous subsequent fluvio-deltaic deposition in the Kutei Basin (Tanean et al., 1996). The Mahakam River incised the Samarinda

anticlinorium during the middle Miocene and successive deltas have since prograded from a single point source near the present delta apex (Allen and Chambers, 1998; Payenberg et al., 2003). The long-term subsidence rate of the lower Kutei Basin is estimated at 0.2–0.5 m/ky (Roberts and Sydow, 1996, 2003).

Three major deltaic complexes, separated by two marine transgressions, characterise deposition in the lower Kutei Basin since the lower Miocene. These complexes are dated as middle Miocene, Miocene–Pliocene, and Holocene (Trevena et al., 2003). The Miocene–Pliocene deltaic sequences have been extensively described by Trevena et al. (2003) and consist of various phases of delta development represented by heterogeneities in the deposits caused by different climate regimes and tectonic uplift of the catchment area. The most recent progradational phase of the Mahakam delta started about 5000 yr BP (Caratini and Tissot, 1988; Comabaz and Matharel, 1978) and continues up to the present day.

2.2. River system characteristics

The present Mahakam River drains about 75,000 km^2 of the (upper) Kutei Basin as well as part of the uplifting central Kalimantan ranges. From available rainfall data and the size of the drainage basin, a mean water discharge was evaluated by Allen and Chambers (1998) of the order of 3000 $m^3\ s^{-1}$ with large seasonal variations. Floods of up to 5000 $m^3\ s^{-1}$ may occur in the upper and middle reaches of the catchment, which is separated from the river mouth of the drainage basin by a subsiding area characterized by a low relief alluvial plain and several large lakes, located some 150 km upstream of the delta plain (Roberts and Sydow, 2003). The lakes create a buffer causing the dampening of the flood surges (Allen and Chambers, 1998) and effectively level off Mahakam River floods, resulting in a constant discharge for lower reaches of the Mahakam River and delta system.

The absence of peaks in river discharge has resulted in a delta plain that has no natural levees or crevasse splays. Therefore, avulsions of distributary channels do not take place. Instead, as the delta prograded, bifurcations of the fluvial distributaries occurred about every 10 km. The climatic conditions are tropical, with only a slight monsoon impact. Rainfall ranges from about 4000 to 5000 mm per year in the central highlands to 2000 to 3000 mm per year near the coast (Roberts and Sydow, 2003) and has a high in January and a low in August. Temperature shows little interannual variation and is on average 25.5 °C. The average sediment discharge is estimated at $8*10^6\ m^3\ yr^{-1}$ (Allen et al., 1977), although this number is not based on actual field measurements but on volumetric calculations.

2.3. Marine processes

The tides in the Strait of Makassar are semi-diurnal with a considerable diurnal inequality. Tidal amplitude ranges from less than 1 m in neap tides to about 3 m during spring tides that occur with a 15 day periodicity (Allen and Chambers, 1998). Although these tide amplitudes are not very large compared to macro tidal amplitudes, they are sufficient to generate strong tide-induced currents which lead to reversing the flow direction of the Mahakam River as far upstream as Samarinda, located about 20 km upstream from the delta apex. The wave energy that affects the delta is very low. Low wind speeds and the small fetch in the Makassar Strait result in a significant wave height of less than 0.6 m (Roberts and Sydow, 2003). Furthermore, the shallow submerged delta-front platform, which extends to the 5 m isobath several kilometres offshore (Fig. 2), dissipates wave energy so that only low-energy waves reach the coastline. Wave direction varies from north to southeast. The Makassar Strait is subject to a southern throughflow that generally persists throughout the year (Murray and Arief, 1988).

2.4. Delta morphology

The modern Mahakam delta (Fig. 2) forms a regular fan-shaped lobate system with a thickness around 50 to 70 m. It covers about 1800 km^2 of predominantly subaerial delta plain and about 2000 km^2 of delta-front platform and delta-front slope accumulations (Allen et al., 1977). During the past 5000 yr, the delta plain has prograded up to 60 km over older Holocene transgressive deltaic deposits (Roberts and Sydow, 1996). The modern Mahakam has two active fluvial distributary systems directed northeast and southeast. The intervening areas consist of tide-dominated areas, with many high sinuosity channels which are mostly not connected to the fluvial system (Fig. 2). This inter-distributary zone occupies approximately 30% of the delta plain (Allen et al., 1977).

The delta-front platform consists of a shallow (<5 m water depth) intertidal to subtidal platform fringing the densely vegetated lower delta plain (Fig. 2). The width of the delta-front platform varies between 10 and 20 km and its outer limit is marked by a strongly inclined slope seaward of the 5 m isobath (Allen et al., 1977). The delta-front platform contains subaqueous channels

(Lambert, 2003), which prolong both the tidal channels and fluvial distributaries. The delta-front platform environment is the area of continuous interplay between tidal and fluvial processes, which has led to a complex depositional pattern ranging from fluvial related sandy bars to tide-related mud, which will be more extensively discussed later in this paper.

The delta-front slope is located beyond the 5 m isobath and marks a sharp increase in sea bottom slope. The outer limit of the delta-front slope is estimated at a water depth of around 70 m where it passes into the prodelta. Deposition on the delta-front slope consists of suspended silt and clay (Allen et al., 1977). The bathymetry of the shelf (Fig. 2) clearly shows rough bottom bathymetry that is formed by individual and aggregated mound-like bioherms (Roberts and Sydow, 1996; Wilson and Lokier, 2002). These bioherms (Halimeda calcareous alga) can be up to 20 to 30 m thick and are located on a regional erosion surface that separates the latest Pleistocene deposits from the modern Mahakam prodelta deposits (Fig. 3) (Roberts and Sydow, 2003). As sediment from the Mahakam is preferentially transported in southerly direction due to a north to south directed longshore current (Murray and Arief, 1988), the reefal build ups in the north appear to be close to the prodelta (~20 km), whereas in the south they are much further away (~40 km) (Magnier et al., 1975).

The Mahakam delta plain is densely vegetated, with three vegetation zones indicating the relative elevation of the land to sea level (Fig. 2). A mixed-hardwood forest characterises the well-drained supratidal upper delta plain and extends about 10 to 20 km from the landward limit of the delta. The upper delta plain has a low flooding frequency and therefore a low deposition rate. The lower delta plain is vegetated with *Nypa* palms and mangroves. The mangrove forest colonises newly formed intertidal flats and is very successful in trapping fine-grained sediment. As soon as the intertidal flat reaches a higher elevation, the mangrove forest is replaced by the characteristic *Nypa* palms.

3. Data collection

In September 2003 a two-week field campaign was conducted in the Mahakam delta plain using a hand-augering device for onshore coring and a small speed-boat for logistics. This enabled us to disembark at any place along the river and core in densely vegetated areas. A total of 28 cores (Fig. 4) were collected with a maximum depth of 8.5 m and a core diameter of 3 cm. Hand-augering is a fast and easy-to-use method to recover a continuous subsurface sediment sample of 1 m length in unconsolidated sediments ranging in grain size from clay to fine sand, but is not capable of penetrating into coarser sediments below the ground water table. This problem has at times limited the coring depth. The cores were described in the field, assessing grain size, organic content, macrofossils and colour. 22 samples were collected for AMS ^{14}C dates (Table 1). To decrease the possibility of sampling reworked organic material, we collected predominantly

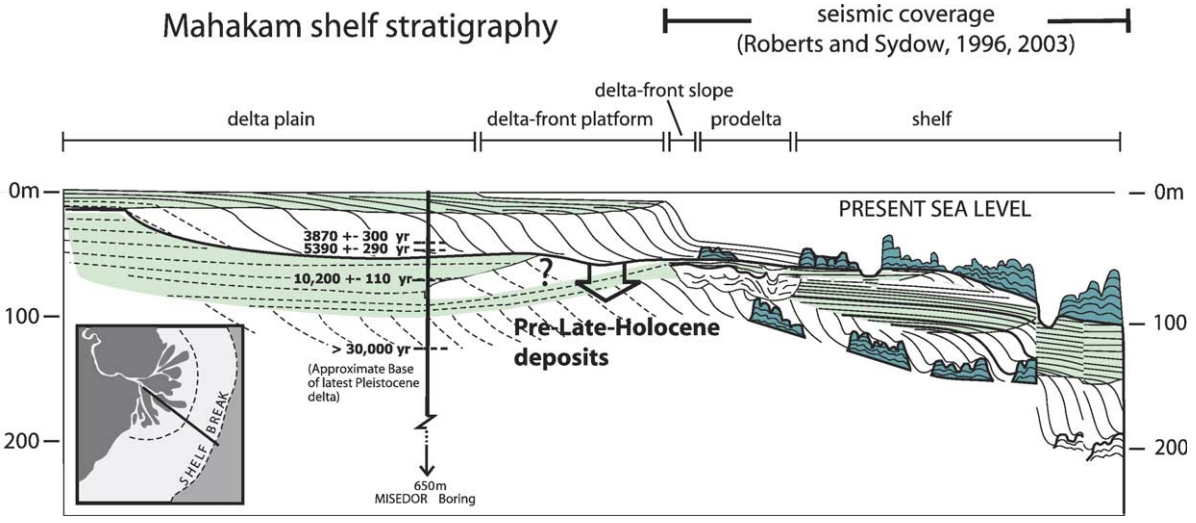

Fig. 3. A schematic representation of pre-Holocene and Holocene Mahakam stratigraphy (modified after Roberts and Sydow, 2003) with MISEDOR core (Carbonel and Moyes, 1987) location and main time and depth boundaries of important Pleistocene and Holocene surfaces. In the offshore zone several carbonate bioherm structures are situated, which are remains of the late Pleistocene–early Holocene transgressive phase.

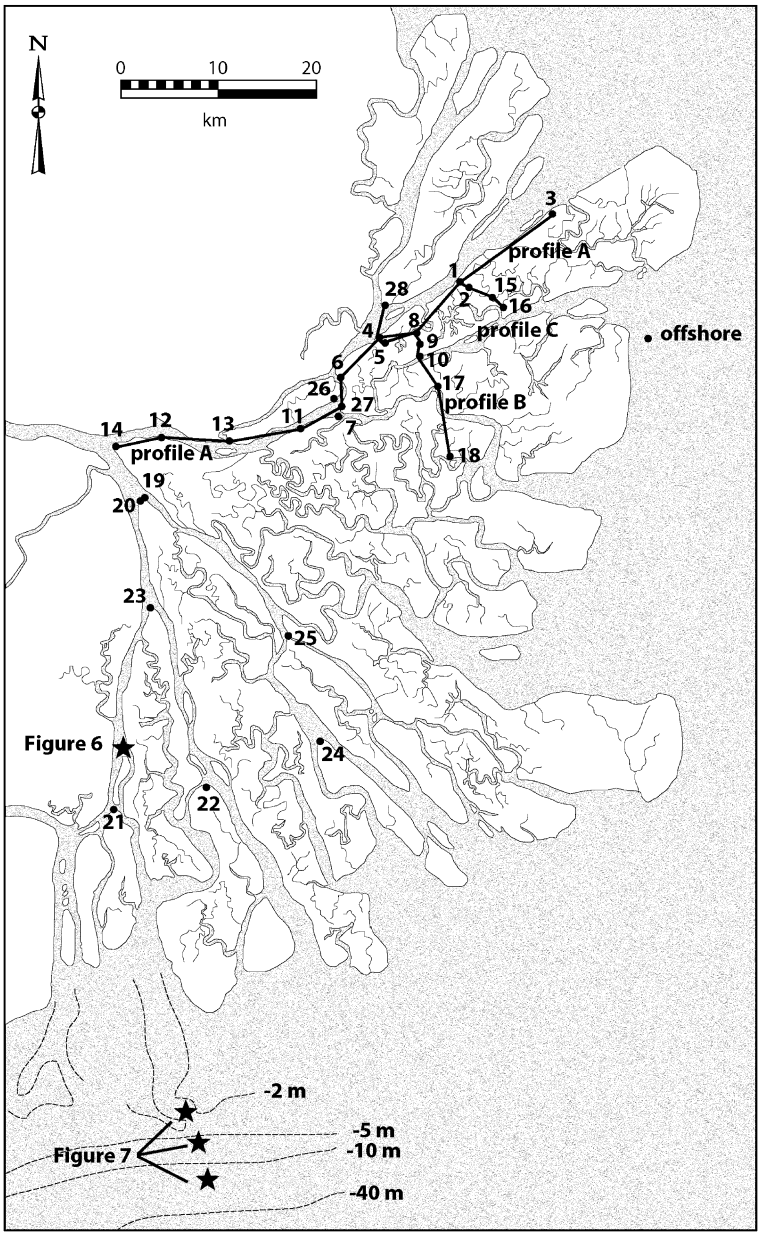

Fig. 4. Map showing core locations and associated cross-sections, and the locations of the acoustic Doppler current meter measurements presented in Figs. 6 and 7, with the isobaths in the vicinity of these measurements.

soft fibres from *Nypa* palms, which were easy to identify. In four cases we collected wood samples. A differential GPS system was used for determining the core position. This worked well and determined the horizontal position of the coring-locations, within a 1 m radial resolution. The GPS measurements did not provide adequate vertical positioning. Therefore, it was assumed that the topographic features in the delta plain are negligible and that a very slight sloping topography from apex to the delta-front prevails.

Shipboard measurements were taken from the Geomarin research vessel. For current velocity observations the vessel was equipped with a broad-banded 1.2 MHz Acoustic Doppler Current Profiler (ADCP), manufactured by RDI. The ADCP transmitted 8 pings per ensemble along four beams, at an angle of 20° to the vertical. The depth cell size was set at 0.25 m. Stratification of water masses was investigated using a Seabird CTD (Conductivity Temperature Depth) probe, which sampled synchronously with the ADCP observa-

Table 1
Calibrated ^{14}C AMS dates in calendar years with interpreted facies types (DP = delta plain, TDDF = tidal dominated delta-front platform, FDDF = fluvial-dominated delta-front platform, LCB = lateral channel bar, MB = mouth bar)

Number	Sample location	Depth [cm]	Calibrated age [yr BP]	± Error margin [yr]	Comments	Analysed fraction	Facies
MD1	Core 7	430	1710	97	Contaminated	Wood	LCB
MD2	Core 7	590	2263	81		*Nypa* fibre	LCB
MD3	Core 8	270	3103	102		Wood	DP
MD4	Core 8	610	3813	89		*Nypa* fibre	FDDF
MD5	Core 8	845	4218	127		*Nypa* fibre	FDDF
MD6	Core 9	785	4220	66		Marine shells	FDDF
MD7	Core 10	375	696	30		*Nypa* fibre	LCB
MD8	Core 10	830	1240	53		*Nypa* fibre	LCB
MD9	Core 11	465	3384	52		*Nypa* fibre	FDDF
MD10	Core 12	135	3420	39	Contaminated	Wood	DP
MD11	Core 12	320	3286	72		*Nypa* fibre	FDDF
MD12	Core 13	510	2535	173		*Nypa* fibre	LCB
MD13	Core 14	180	0	0	Modern	*Nypa* fibre	LCB
MD14	Core 14	330	0	0	Modern	*Nypa* fibre	LCB
MD15	Core 15	635	806	78	Too young?	Wood	?
MD16	Core 20	193	231	226		*Nypa* fibre	Top MB
MD17	Core 22	180	358	71		*Nypa* fibre	Top MB
MD18	Core 23	243	826	84		*Nypa* fibre	Top MB
MD19	Core 24	278	362	68		*Nypa* fibre	Top MB
MD20	Core 27	426	3236	154		*Nypa* fibre	FDDF
MD21	Core 27	445	1150	79	Contaminated	Wood	FDDF
MD22	Core 28	235	2396	68		*Nypa* fibre	TDDF

For core location see Figs. 4 and 9.

tions. The CTD casts were taken using a winch on the research vessel. Vertical profiles of salinity were obtained using the upcasts only, which covered the entire water column except for the bottom 50 cm. A Seapoint Optical Backscatter sensor (OBS) was attached to the CTD probe. For the OBS measurements, only the downcasts were used, as the CTD probe could create some sediment clouds when it touched the seabed. For calibration purposes, a Niskin bottle was attached parallel to the CTD to collect in situ water samples. The suspended sediment content (SSC) of the water samples was measured by vacuum filtration of a fixed amount of water on pre-weighed polycarbonate filters with a pore size of 0.4 μm. After filtration, the filters were cleaned with nano-pure water to remove salts, washed with alcohol, and dried and weighed. The regression results of the SSC measurements taken from water samples against OBS voltage are shown in Fig. 5.

Fig. 6 presents time–depth plots for longitudinal current velocity, salinity and suspended sediment concentration over a tidal cycle at an anchor station in the southernmost active river distributary (Fig. 4). It shows that the location is close to the outer region up to which the salt intrusion reaches, with salinities remaining well below 10 PSU. The flood currents are relatively weak because the river discharge is directed oppositely. During flood tide, suspended sediment concentrations gradually decrease roughly from 100 to 50 mg/l, indicating that the entering waters are relatively clear. To some extent, the opposite pattern occurs at the time of the ebb currents, which convey relatively turbid waters from upstream and cause resuspension near the bed. The gradual decrease in suspended sediment concentration during flood tide in the main river distributary indicates a negative downstream turbidity gradient, which is in accordance with regional deposition of alluvial sediments on the delta plain.

Downstream of the river anchor station, river mouth processes were observed by taking CTD/OBS casts

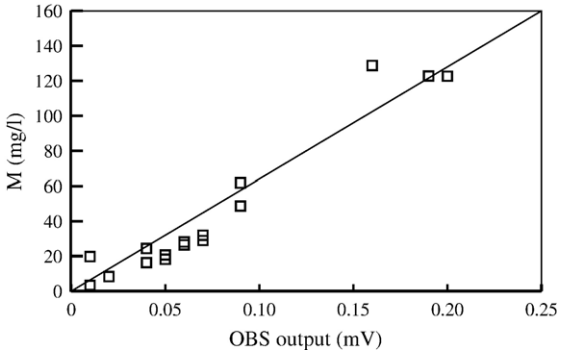

Fig. 5. Plot of the OBS calibration. In situ water samples were taken at various sites in the southern river branch and adjacent river mouth of the Mahakam River.

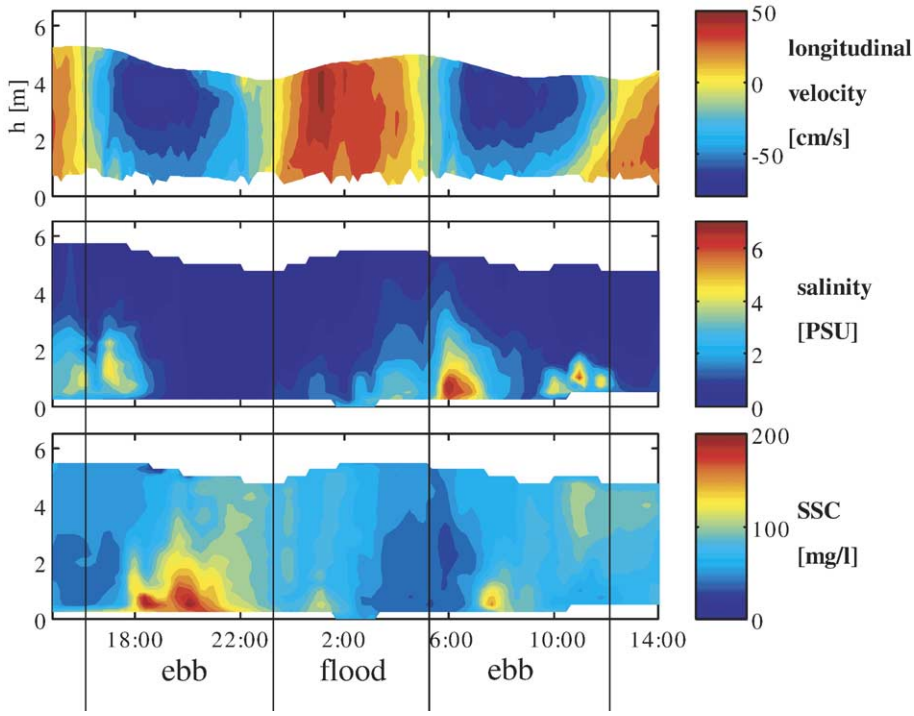

Fig. 6. Measurements of longitudinal flow velocity, salinity and suspended sediment concentration (SSC) at an anchor station about 20 km inland from the river mouth (Fig. 4), indicating a negative downstream turbidity gradient.

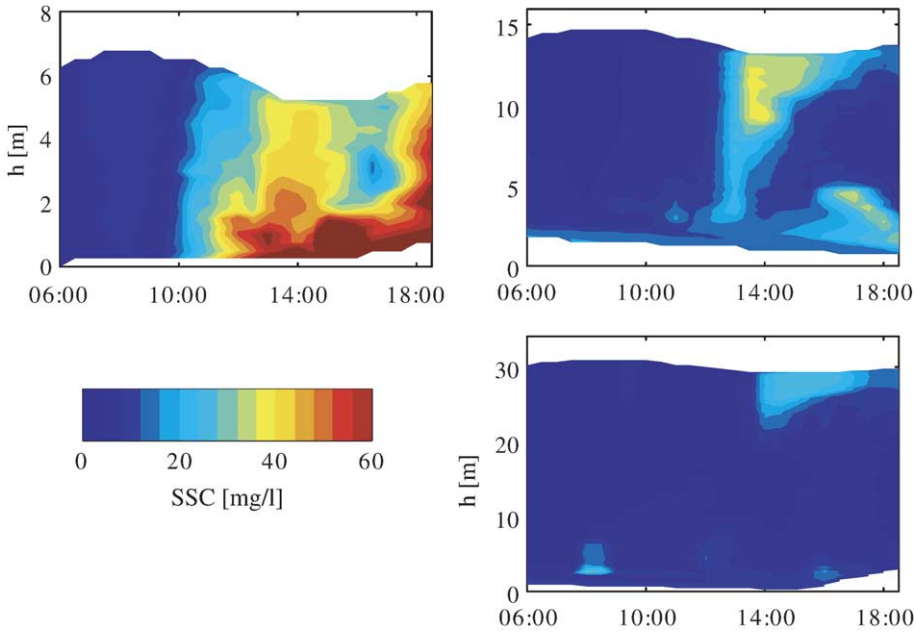

Fig. 7. Quasi-simultaneous observations of the development of a river pulse in front of a distributary channel at the delta-front platform at three locations (6, 14 and 30 m water depth), showing rapid settlement of suspended sediment. See Fig. 4 for location. SSC: suspended sediment concentration.

alternately at three locations on the delta-front platform, respectively in 6, 14 and 30 m water depth (Fig. 4). The measurements lasted for a tidal period about halfway through the spring–neap cycle (Fig. 7). Just before slack water after falling tide, a water mass with a salinity of about 25 PSU progressively migrates seaward, dumping the majority of the sediments between the 6 and 14 m isobaths on the channelised delta-front platform. Peak levels of suspended sediment concentration amounted to 60, 40 and 25 mg/l at the locations at 6, 14 and 30 m, respectively. The observed rapid settlement of the sediments on the delta-front platform illustrates the day-to-day progradation of the delta due to suspended clays and silts. The salinity profile shows that the sediment plume remains intact without mixing with seawater, an indicator of rapid settlement of river sediments.

4. Sediments and stratigraphy of the late-Holocene delta development

Whereas suspended sediments are predominantly composed of silt and clay, bed load sediments are relatively sandy, leading to mouth bar formation (Bates, 1953). At falling tide, flow is directed seawards and sediment is transported towards the mouth bar and delta-front platform. Deposition of sand occurs in a fan shaped manner, with decreasing grain size and quantity as flow competence decreases in an offshore direction (Fig. 8A). The extent of the area of sand deposition is variable; it increases during the ebb phase of neap tide and decreases during the ebb phase of spring tide. Measurements of suspended sediment concentrations directly in front of a main distributary channel indicate that high sediment loads are restricted to the shallow part of the delta-front platform (Fig. 7). Little sediment is transported beyond the 15 m isobath and the background rate of suspended sediment concentration is less than 20 mg/l. This implies that most of the sediment transported by the Mahakam River is deposited in the delta-front platform zone.

Most mouth bars located in front of active Mahakam distributary channels are intertidal and are aerially exposed during low tides. In these cases, the water flows around the mouth bar, thereby increasing the angle of sediment dispersal over the delta-front platform (Fig. 8). According to Allen and Mercier (1994) this eventually will lead to a new bifurcation point of the distributary channel. If, however, the mouth bar is not yet well developed, meaning that its topographic expression is small, then the flow will be directed both over and along the mouth bar, causing it to migrate seawards as well as upward. On the delta plain, flooding water from the previous high tide cycle is drained from the intertidal lower delta plains during falling tide.

During rising tide, flow is directed inland in both the distributary and tidal channels. The rising water level causes the delta plain to be flooded as water is forced into the extensive network of tidal channels and creeks. The mangrove and *Nypa* vegetation traps the clay particles which are suspended in the floodwater. On the delta-front platform, clay deposition is widespread as flow competence is low (Fig. 8A). Mud deposition in the distributary channel is partly driven by the presence of a turbidity maximum in the lower reaches of the distributary channels (Allen and Chambers, 1998).

Sediments from both high and low tide conditions accumulate with a variable degree of erosion or reworking as the delta progrades, which leads to a zonation of five facies types across the delta plain and delta-front platform (Fig. 8B). The facies types are classified according to their average grain size as well as heterogeneities in grain size and colour. The field observations of the grain size were confirmed by analysis of 43 grain size samples taken from core 12, using a laser diffraction spectrophotometer (Konert and Vandenberghe, 1997).

4.1. Facies

Lower delta plain facies (DP) consists of massive clays, deposited onshore in the tidal-dominated interdistributary areas, which are rich in rootlets and have a variable degree of organic content and macrofossils. Sporadically there may be some sand or silt incursions. The thickness of the lower delta plain facies is related to the tidal amplitude. Mangrove starts to colonize tidal flats as soon as they become intertidal. This restricts the thickness of the lower delta plain facies to about 3.5 to 4 m.

Tidal-dominated delta-front platform facies (TDDF) consists of clayey to silty deposits that show distinct colour laminations at millimetre scale. Organic content is low or absent and macrofossils are sparse, root burrows may occur. Deposition typically takes place offshore from the tidal-dominated interdistributary areas away from the river mouth and hence this facies lacks sand inclusions. Nevertheless, the variability in flow regime over the tidal cycles results in millimetre-scale laminations of clay drapes.

Fluvial-dominated delta-front platform facies (FDDF) consist of distinct laminated sand, silt and

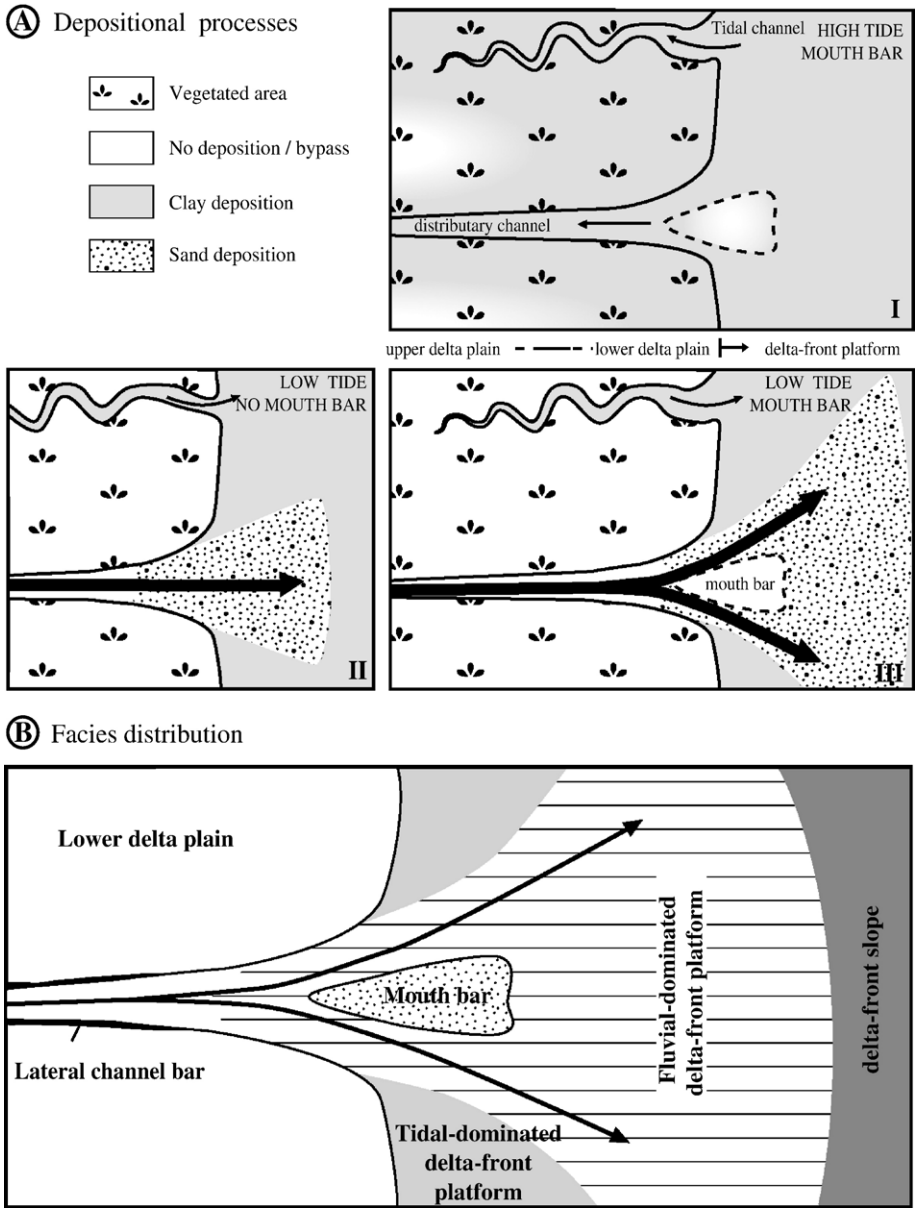

Fig. 8. (A) Schematic representation of the dispersal of sand and clay under varying tidal conditions. During rising tide conditions (I) depositional processes lead to extensive clay deposition. As the tide falls (II and III), sand is dispersed by the fluvial channel in a fan-like shape in the absence of a mouth bar (II) or in the presence of a mouth bar (III). (B) shows a schematic representation of the facies distribution in the Mahakam delta.

clay bands with thicknesses from on average 1 to 5 mm, and sometimes up to a few centimetres. The boundaries between laminae are sharp, however structural trends in the thickness of the laminae as described in other subtidal deposits (Visser, 1980) were not observed. The fluvial-dominated delta-front platform facies originates from flow reversal in the vicinity of the river mouth as sand is deposited during low tide and clay is deposited during high tide conditions. This facies type is directly related to the distributary channel system as the flow capacity in tidal channels is too low to transport sand (Allen et al., 1977).

Lateral channel bar facies (LCB) consist of sand–mud couplets similar to fluvial-dominated delta-front platform facies. Lateral channel bar facies form along the margins of a distributary channel as the channel thalweg slowly changes in time. As such, lateral channel bars are formed and eroded as a function of autocyclic channel behaviour and therefore their age bears no direct relation to the depth of deposition nor with sea

level (Allen et al., 1977; Allen and Mercier, 1994). As a prograding distributary channel erodes underlying older delta-front platform facies, lateral channel bar facies are expected to be considerably younger than surrounding fluvial-dominated delta-front platform facies. Cores that showed lateral channel bar facies were located within

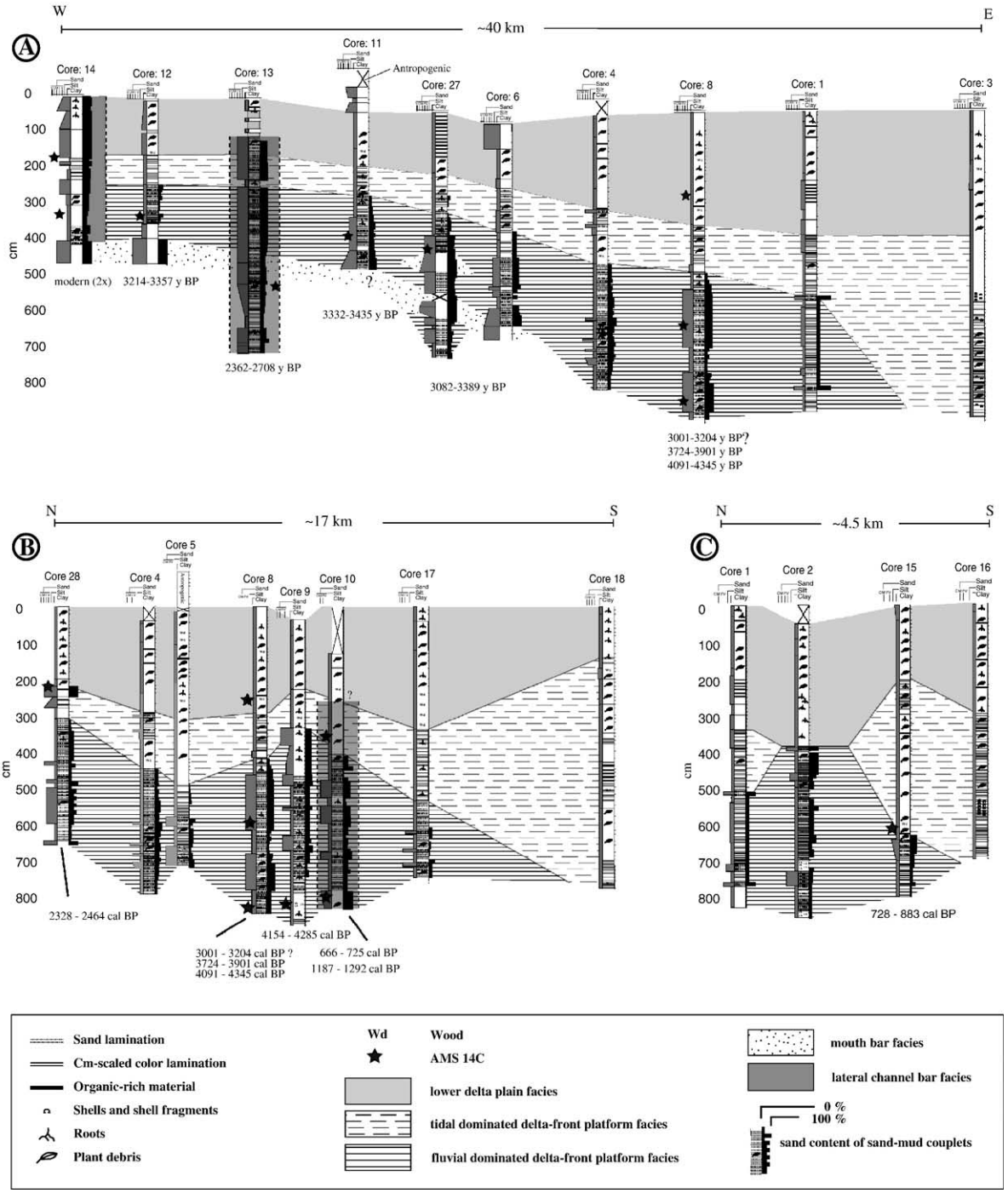

Fig. 9. Three cross profiles constructed using the core-data (Fig. 4 for location). The west–east Profile A shows the thickening of the facies in downstream direction. Profiles B and C are perpendicular to the main channel showing a decrease in sand content towards the tidal dominated area of the delta representing an increase in tidal domination. (See text for further explanation). The positions of calibrated AMS ^{14}C dates are shown using asterisks, the ages are indicated below the core.

several metres from a distributary channel (Fig. 4, core 7, 10, 13 and 14). Although the distributary channels are straight and do not migrate, Allen et al. (1977) pointed out that the channel thalweg does meander. At the inner bend of such thalweg meanders, subaqueous point bar-like features evolve consisting of sand–mud couplets, and which were classified as lateral channel bars facies. The resemblance to fluvial-dominated delta-front platform facies lead Gastaldo et al. (1995) to believe that all sand–mud couplets could be classified as lateral channel bar deposits.

Mouth bar facies (MB) consists of massive, well sorted medium grained sand (>0.25 mm). It occurs directly in front of the distributary channel and therefore consists of much coarser sand and better sorted than the sands in the surrounding fluvial-dominated delta-front platform facies. The mouth bar can build up to intertidal elevation and therefore may be subaerially exposed during low tide. Since our coring technique cannot penetrate these coarse sand bodies, we refer to Allen and Mercier (1994) for a more detailed description of the mouth bar sediments, their evolution and distribution.

4.2. Facies succession

Core data are used to construct three facies profiles (Fig. 9) which give insight into the spatial distribution of the facies successions. Profile A is located along a main northern distributary channel (Fig. 4) and records the progradational history of the delta plain and delta-front platform. The facies succession thickens seawards as accommodation space increases. Mouth bar facies are only present in the western part of the section. During the initial onset of the modern delta progradation, accommodation space was low and the number of distributary channels was restricted. The mouth bars therefore were closely spaced over a relatively small and shallow area. As progradation continued the individual mouth bars became laterally separated by fluvial and tidal dominated delta-front platform facies. These later facies are therefore more pronounced in the eastern cores. The dates suggest that the fluvial-dominated delta-front platform facies ranges in age between 3000 and 4300 yr BP (Table 1; Fig. 9), but four dates are inconsistent. Core 8 (MD3; Table 1) shows a relatively old date from a wood sample that most likely is a reworked wood fragment. The date in core 13 (MD12; Table 1) appears to be too young when compared to dates of neighbouring cores. The high sand content in this core, as well as its location about 3 m from the distributary channel suggests that the deposits originate from a lateral channel bar rather that from delta-front platform deposition. The same pattern can be seen in core 14, where two dates indicate a modern age (MD 13 and MD 14; Table 1).

The two remaining profiles of Fig. 9 are situated perpendicular to the main distributary channel (Fig. 4). These cross profiles show the transition from a fluvial-dominated to a tidal-dominated delta-front platform depositional environment. Neither of the two profiles shows mouth bar facies, which is consistent with the distribution of mouth bar facies shown in profile A. The tidal-dominated delta-front platform facies shows a significant increase in thickness towards the tidal-dominated domain. The absence of the tidal-dominated delta-front platform facies in core 2 (Profile C) may be due to local conditions. Both profiles show a decrease in sand content towards the tidal dominated depositional environment as is expected based on the proposed sediment dispersal pathways shown in Fig. 8. The thickness of the delta plain deposit has a maximum of 4 m and does not increase or decrease systematically. The AMS ^{14}C dates (Table 1) in profile B are consistent with those of profile A except for the two dates retrieved from core 10 (MD7 and MD8; Table 1), which are relatively young. This core is positioned along a wide and low sinuous tidal channel. In contrast to other tidal channels it has a narrow connection to the fluvial system. Channel morphology and the relatively young age imply that this channel may in fact be a former distributary channel, which suggests that the encountered sand–mud couplets are lateral channel bar facies rather than a fluvial-dominated delta-front platform facies. Data from core 10 indicate that this channel is an old fluvial distributary, which is in the process of being transformed into a tidal channel. According to Allen et al. (1977) such transitions are not uncommon, especially in the northern distributary system, since this distributary system is in the process of abandonment (Allen and Chambers, 1998). Nevertheless, recent satellite images show that high concentrations of suspended sediment are discharged from the northern distributary channels during low tide (Budhiman, 2004).

5. ^{14}C dates versus eustatic sea level history

No data exist on late Holocene sea level change for eastern Kalimantan or the Strait of Makassar. Although the new ^{14}C dates from this study have a low vertical resolution, as the topographic elevation could not be accurately determined, the dates can still be used to get a first impression of late Holocene sea level. For each

facies type except the lateral channel bar facies, we know approximately at what water depth deposition took place. For example, we assume that a distributary channel bifurcates if the associated mouth bar grows high enough vertically to reach the intertidal zone. Distributary channel bifurcations take place every 10 to 20 km in the delta and occur in both the northern and the southern distributary system. As soon as the mouth bar reaches the intertidal zone, which has a direct relation to mean sea level, it becomes vegetated and delta plain deposits will cover the intertidal mouth bar. The depth in the core at which this transition occurs has a direct relation to mean sea level and can be dated. In the same manner, delta plain and delta-front platform facies can be used as a proxy for sea level history. As lateral channel bar deposition is related to channel dynamics rather than sea level, those dates could not be used.

Fig. 10 shows a diagram of the ^{14}C dates versus depth. The carbon dates are compared to the eustatic sea level curve of Fairbanks (1989), which give a first approximation for the late Holocene sea level history of an otherwise well studied delta system. We excluded the dates from cores that are interpreted to originate from lateral channel bar accretion (MD1, MD2, MD7, MD8, MD12, MD13 and MD14; Table 1) as well as erroneous dates (MD3, MD10 and MD21; Table 1). These latter dates were either based on reworked wood samples (MD3 and MD10; Table 1) or were contaminated (MD21; Table 1). Fig. 10 suggests that sea level has risen between 4500 cal yr BP and present. The data suggests a fairly good fit with an exponential sea-level curve, where the fastest sea level rise took place between 4500 and 2500 cal yr BP. This suggests that sea level history in Eastern Kalimantan may not differ much from the eustatic sea level history (Fleming et al., 1998). The average subsidence rate estimated by Roberts and Sydow (1996, 2003) between 0.2 and 0.5 mm yr^{-1} fits the data presented here, but it should be noted that the vertical resolution of the depth measurements is not sufficient to refine the subsidence estimates. Furthermore, there is no indication to suggest that there was a local Holocene sea-level highstand as seen in the nearby Sunda Shelf deposits (Hanebuth and Stattegger, 2004).

6. Deposition rates

Two ^{14}C dates in core 8 (MD4 and MD5; Table 1), both representing fluvial dominated delta-front platform facies, were used to calculate an average deposition rate of 10.9 mm yr^{-1}. On average there are 2 to 5 sandy layers per vertical centimetre of fluvial-dominated delta-front platform facies which are separated by mud layers. In general, sand beds are deposited during low-tide conditions (Fig. 8A). Although the variability in sand bed frequency and thickness is large, it implies that on average each year deposits related to 2 to 5 individual ebb occurrences are preserved. The number of preserved sand beds per vertical unit is governed by the number of deposition events and the number of erosion events. The probability of sand deposition (both thickness and frequency) at a location near the river mouth increases with the tidal amplitude. The highest probability for sand deposition at the fluvial dominated delta-front platform therefore occurs during ebb stage of spring tides, when river flow velocity is highest. It is not clear if sand is deposited at the delta-front platform during ebb stage with smaller tidal amplitudes. The role of erosion cannot be estimated but observations indicate that preserved beds have sharp boundaries and show no grading trends within

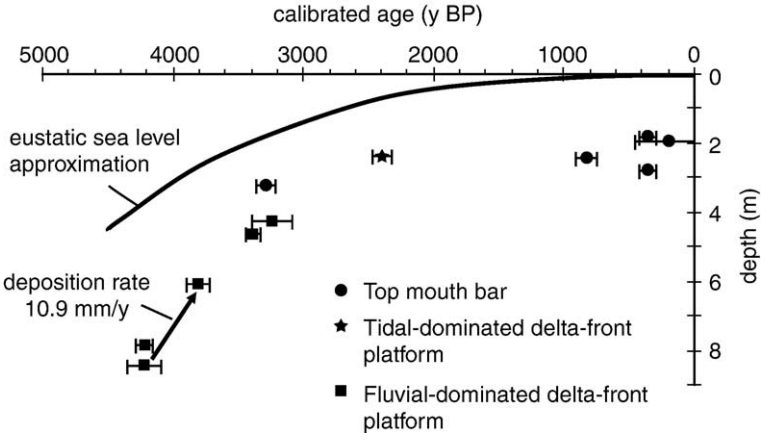

Fig. 10. Comparison between eustatic sea level (Fairbanks, 1989) and AMS ^{14}C dates of various depositional environments in the Mahakam delta.

the beds. This implies that (some) erosion takes place, removing either the complete sand layer or just the top. Based on the above, we argue that the fluvial-dominated delta-front platform deposits consist predominantly of ebb stage deposits related to spring tides.

The deposition rate for lateral channel bar facies, calculated using ^{14}C dates in cores 7 (MD 1 and 2; Table 1) and 10 (MD 7 and MD 8; Table 1), is respectively 9.7 and 10.4 mm yr^{-1}. Because the layer thickness for the lateral channel bar facies is comparable to the fluvial-dominated delta-front platform facies, this implies that these sand–mud couplets may also represent neap–spring tide cycles, as suggested by Allen et al. (1977) and Gastaldo et al. (1995). However, we would expect that the rate of erosion along a distributary channel would be higher and more variable than at the delta-front platform.

7. Discussion

The data presented in this paper give a first impression of the lateral extent of the different depositional environments and their variability in a mixed fluvial–tidal delta system. The trends in facies succession are consistent through the constructed cross-sections as well as the new ^{14}C dates. There is a seawards decrease in sand content in the uppermost 8 m, caused by the downward dip of the facies successions. The decrease in sand content in a cross-shore direction is a result of decreasing flow competence. Within the fluvial dominated delta-front platform facies, we did not notice a trend in either sand–mud ratio or thickness of the couplets, which is in contrast with the findings of Gastaldo et al. (1995) who noticed an overall increase in the sand–mud ratio of the couplets in a downstream direction. Allen and Chambers (1998), however, reported a downstream fining trend in some of the cores taken in the Mahakam distributaries. The ambiguous data may be explained by the fact that cross channel variability in facies succession is important (Fig. 9; profile B and C) as well as making a distinction between the lateral channel bar facies and fluvial dominated delta-front platform facies. The latter two facies look identical but are genetically very different and therefore should not be compared in terms of sand content. Our data suggest that the two facies types consisting of sand–mud couplets can only be distinguished based on the radiocarbon dates.

At present, there are eight active distributary channels entering the Strait of Makassar in the south and four in the north. For each new bifurcation point, the discharge is divided over the two newly formed distributary channels. A large number of coexisting distributary channels causes a relatively low discharge per distributary channel. Under invariable tidal conditions, this implies that the balance between fluvial and tidal processes shifts slightly to tidal-domination for each new bifurcation, so that deposition generally becomes more clay rich. Assuming that both river discharge and tidal character did not change significantly during the past 5000 yr, one would expect a shift from a fluvial dominated to a tidal dominated delta system as progradation continued. Also, during the onset of progradation, very little accommodation space was present for tidal infill and the distributary mouth bars are therefore closely spaced, possibly even interconnected. As progradation continued each bifurcation led to an increase in tidal accommodation as the radius of the delta increased.

Allen et al. (1977) suggested that the tidal processes have a dampening effect on the fluvial dynamics of the delta, which they use as an argument to explain the lack of typical fluvial deltaic features such as levees and crevasses. As the influence of the tidal processes increased in time while the delta prograded, the absence of any crevasses or natural levees suggests that the specific non-flooding discharge regime of the lower Mahakam catchment area has led to their absence, rather than tidal dampening (Bryant et al., 1995). This is also suggested by the fact that there appears to be virtually no channel migration in the delta plain. Analysis of aerial photos from 50 years ago has shown no significant changes in channel locations (Allen et al., 1977).

The presence of lateral channel bar facies does suggest either channel migration or narrowing and infilling of the channel. The first has not been observed because both tidal and distributary channels appear to be very stable. Nevertheless, four cores (7, 10, 13 and 14), positioned directly along a channel, show lateral channel bar facies. A closer look at the core location map (Fig. 4) shows that these cores are positioned along a relatively narrow, meandering channel which appears to be tidal in origin, but which still has a narrow connection to the distributary channels. As tidal channels are not capable of transporting sand (Allen et al., 1977), the presence of sand–mud couplets indicates that some tidal channels once were distributaries but later converted into tidal channels.

The volume of the late-Holocene Mahakam delta is estimated to be 200 km^3. This number is calculated based on the sum of the aerial extent of the delta plain (~1800 km^2) and the delta-front platform (~2000 km^2), multiplied by the average delta thickness (50 m for the

delta plain and 45 m for the delta-front platform; Caratini and Tissot, 1988; Roberts and Sydow, 2003). This volume of sediment has been deposited during the past 5000 yr. Based on the suspended sediment measurements in the main southern distributary channel (Fig. 6) it is estimated that the sediment load is about 150 mg/l. Allen and Chambers (1998) estimated the water discharge to be in the order of 3000 m^3 s^{-1}. This would imply that the volume of suspended sediment deposited over a 5000 yr period would be about 26 km^3. Adding a rough estimate for bed load as 10% of the suspended sediment load (Syvitski et al., 2003) brings the total volume to 30 km^3. The present-day supply of sediment is clearly too low to have resulted in the formation of the late-Holocene Mahakam delta complex. Although the present-day water and sediment discharges are only rough estimates, it would be unrealistic to increase either of them by a factor of six to explain the actual volume of the present Mahakam delta. The offset between delta volume and present-day sediment load may indicate that there have been different hydraulic conditions in the past. Although there have continuously been lakes present upstream from the Mahakam delta during the course of the Holocene, their influence on the downstream Mahakam River may have varied in time. In the absence of regulating lakes, river floods, which are presently absent in the delta, may have transported considerable amounts of sediment to the delta. However, river floods also would have created levees and crevasse splays, and no evidence has been found for their existence. Considering the location of the delta at the Equator, it is unlikely that the climatic conditions have changed much during the late Holocene, leading to changes in sediment discharge. Additional ^{14}C dates may reveal changes in progradation rate through time, which may be related to varying water and sediment discharge in the past. The relatively dilute present-day river discharge is effective at conveying the limited sediments through the distributary channels with little loss and therefore there is limited infilling of the channels. This latter as well as the lack of river floods may explain the absence of channel migration.

The typical delta-front platform and slope of the Mahakam delta can be interpreted as a subaqueous delta which reveals a compound-clinoform development. Unfortunately, no data exist on the progradation rate of the Mahakam delta-front slope, but observations from other subaqueous deltas such as the Amazon delta (Nittrouer et al., 1996), the Ganges–Brahmaputra delta (Kuehl et al., 1997), the Fly river (Harris et al., 2004) and the Po delta (Cattaneo et al., 2003), suggest that the depositional mechanisms of the subaerial delta and the subaqueous delta may be very different. Subaqueous deltas are commonly attributed to energetic marine environments (Swenson et al., 2005), which are related to energetic waves and large tidal ranges. Fig. 11 shows a comparison between the Mahakam delta and other deltas with compound clinoform development. Each subaqueous delta is different in size due to differences in the river discharge and shelf bathymetry. Yet, the shape of the subaqueous delta is above all formed by the local oceanographic regime. Based on the morphology of the subaqueous delta, a distinction can be made between the delta-front slope and the prodelta/shelf environment (Fig. 11). Fig. 11 shows that the shape of the normalized subaqueous deltas may either be smoothly curved (Amazon, Yangtze and Red River delta) or angular shaped (Mahakam, Ganges–Brahmaputra and Fly River delta). The normalized profile of the Ganges–Brahmaputra delta front is fairly similar to the normalized Mahakam delta front profile. This fairly qualitative analysis shows that the Mahakam delta has a well developed subaqueous delta.

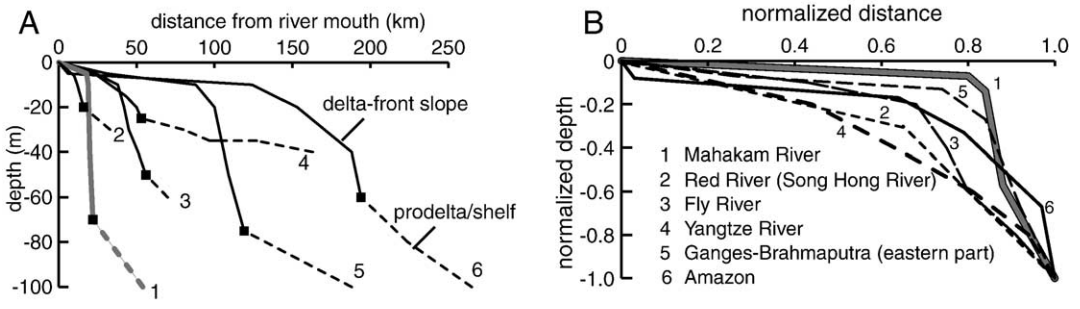

Fig. 11. A: Bathymetric profiles of subaqueous deltas (delta-front, prodelta, shelf) based on bathymetric maps from literature (Harris et al., 2004; Hori et al., 2002, 2004; Michels et al., 1998; Nittrouer et al., 1995; Tanabe et al., 2003). B: bathymetric profiles of subaqueous deltas normalized between the shoreline and the base of the subaqueous delta (bottom set; black square in the top panel). Wave and tidal data of the subaqueous deltas are shown in Table 2.

Table 2
Wave and tidal data based on literature for the Red river delta (Tanabe et al., 2003), Fly River delta (Harris et al., 2004), Yangtze delta (Hori et al., 2002), Ganges–Brahmaputra delta (Michels et al., 1998; Mahboob-ul-Kabir et al., 2002) and Amazon delta (Nittrouer et al., 1995; Sternberg et al., 1996)

	Tidal range (m)		Wave height (m)	
	Mean	Max	Mean	Max
Mahakam	3	?	<0.6	?
Red River	2.0–2.6	3.2–4.0	0.9	5
Fly River	3.5	>5	0.8–1.2	2.9–3.5
Yangtze	2.7	4.6	0.9	6.2
Ganges–Brahmaputra (east)	4.0	6.0	1.6	2.9
Amazon	?	2.9–3.2	1–2	>3

Based on published tide and wave data of these deltas (Table 2) it cannot be determined whether waves or tides are responsible for the curved or the angular shape of the subaqueous delta. Yet, the shallow depths of the delta-front platform of the Mahakam delta may well be attributed to the low wave energy in the strait of Makassar as tropical storms are very rare. As a consequence, sediments deposited in water depths exceeding 5 m are not reworked.

In terms of reservoir geometry, the sand-rich fluvial dominated delta-front platform, the mouth bar and the lateral channel bar facies can be interpreted as one continuous reservoir with a maximum porosity in the mouth bar facies, which are flanked by lower porosity sand–mud couplets. Because the mud couplets are not continuous (Gastaldo et al., 1995), fluid flow is possible in a vertical direction as well as in a horizontal direction. All sand-rich deposits are capped by impermeable delta plain deposits. Roberts and Sydow (1996, 2003) showed the presence of continuous progradational (highstand to lowstand) pre-Holocene sediment wedges, which are in many respects similar to the present delta (Allen and Chambers, 1998). Incised channels that form during the falling sea level (Roberts and Sydow, 2003) dissect the continuous character of the sand-rich deposits. But if the incised valleys are sand-based, as is the case with the present channels (Allen et al., 1977; Allen and Mercier, 1994; Gastaldo et al., 1995; Gastaldo and Huc, 1992), they may enhance the fluid flow properties of the reservoir.

8. Conclusions

- Detailed analysis of new borehole data as well as new ^{14}C dates reveal the late-Holocene evolution of the Mahakam delta. Due to the predominance of semi-diurnal tides and the associated flow reversals, depositional patterns are highly variable which has resulted in the formation of characteristic sand–mud couplets. The distribution of the sand–mud couplets found in this study differs from previously proposed conceptual models. Based on facies analysis, a qualitative depositional model is proposed that explains the sand and clay distribution across the Mahakam delta.
- Calculated averaged deposition rates of the sand–mud couples indicate that deposition of the *tidal-dominated delta-front platform facies* is driven by the spring–neap tide cycles instead of the daily tidal cycle.
- The new ^{14}C dates fit the eustatic sea level curve of the late Holocene, although the vertical resolution of the dates is in the order of 1 m. However, there is no indication for a late-Holocene sea level highstand as has been reported in other studies across southeast Asia.
- Suspended sediment measurements reveal a surprisingly low concentration of sediment in the water column. The present day sediment load of the Mahakam River is insufficient to explain the sediment volume of the Mahakam subaerial and subaqueous delta. This may suggest that the hydraulic conditions in the past may have been different. In addition, the dilute discharge may explain the absence of channel infilling resulting in extremely stable distributary and tidal channel positions.
- Comparison with other tropical deltas reveals that the Mahakam delta has a distinct subaqueous delta morphology that is proportional to the subaqueous delta of the Ganges–Brahmaputra.

Acknowledgements

This project was financed by NWO-WOTRO within the framework of the pilot phase of the East Kalimantan Project (EKP). Co-funding came from EUROSTRATAFORM (contract no. EVK3-CT-2002-00079) for J.E.A. Storms, from the DIOC-program of Delft University of Technology (DUT-DIOC 1.6) for R.M. Hoogendoorn and from the Society for the Advancement of Research in the Tropics (Treub) for A.J.F. Hoitink. ^{14}C AMS datings were processed and analysed by Klaas van der Borg at the R.J. Van de Graaff laboratory of Utrecht University. Martin Konert from the Vrije Universiteit, Amsterdam, assisted with the grain size analysis at the Sedimentology Laboratory. We thank Jan Sopaheluwakan of LIPI, Jakarta for his efforts to initiate the East Kalimantan Coastal Studies project as well as the management of the Geological Research and Development

Centre, Bandung for their support to make the reconnaissance survey possible. Steve Goodbred and an anonymous reviewer and Editor Keith Crook are thanked for their valuable suggestions on an earlier version of the manuscript. Finally we like to mention the crew of the RV Geomarin and our speedboat captain, who guided us through the wilderness of the Mahakam delta.

References

Allen, G.P., Mercier, F., 1994. Reservoir facies and geometry in mixed tide and fluvial dominated delta mouth bars: example from the modern Mahakam delta (East Kalimantan). Proceedings Indonesian Petroleum Association, IPA94-1.1-189, 23rd Annual Convention, October 1994, pp. 261–273.

Allen, G.P., Chambers, J.L.C., 1998. Sedimentation in the Modern and Miocene Mahakam delta. Jakarta, Indonesian Petroleum Association, Field Trip Guidebook, p. 236.

Allen, G.P., Laurier, D., Thouvenin, J., 1977. Sediment distribution patterns in the modern Mahakam delta. Proceedings Indonesian Petroleum Association, vol. 5, pp. 159–178.

Bates, C.C., 1953. Rational theory of delta formation. Bulletin of the American Association of Petroleum Geologists 37, 2119–2162.

Bryant, M., Falk, P., Paola, C., 1995. Experimental study of avulsion frequency and rate deposition. Geology 23, 365–368.

Budhiman, S., 2004. Mapping TSM concentrations from multisensor satellite images in turbid tropical coastal waters of Mahakam delta, Indonesia. Earth resources and environmental geosciences. Enschede, ITC, MSc Thesis. http://www.itc.nl/library/Papers_2004/msc/ereg/syarif_thesis.pdf.

Cattaneo, A., Correggiari, A., Langone, L., Trincardi, F., 2003. The late-Holocene Gargano subaqueous delta, Adriatic shelf: sediment pathways and supply fluctuations. Marine Geology 193, 61–91.

Caratini, C., Tissot, C., 1988. Paleogeographical evolution of the Mahakam delta in Kalimantan, Indonesia during the Quaternary and late Pliocene. Review of Palaeobotany and Palynology 55, 217–228.

Carbonel, P., Moyes, J., 1987. Late Quaternary paleoenvironments of the Mahakam delta, Kalimantan, Indonesia. Palaeogeography, Palaeoclimatology, Palaeoecology 61, 265–284.

Comabaz, A., Matharel, M., 1978. Organic sedimentation and genesis of petroleum in Mahakam delta, Borneo. American Association of Petroleum Geologists Bulletin 62, 1684–1695.

Fairbanks, R.G., 1989. A 17,000-year glacio-eustatic sea level record; influence of glacial melting rates on the Younger Dryas event and deep-ocean circulation. Nature 342, 637–642.

Fleming, K., Johnston, P., Zwartz, D., Yokoyama, Y., Lambeck, K., Chappel, J., 1998. Refining the eustatic sea-level curve since the Last Glacial Maximum using far- and intermediate-field sites. Earth and Planetary Science Letters 163, 327–342.

Galloway, W.E., 1975. Process framework for describing the morphologic and stratigraphic evolution of deltaic depositional systems. In: Broussard, M.L. (Ed.), Deltas, Models for Exploration. Houston Geological Society, Houston, TX, pp. 87–98.

Gastaldo, R.A., Huc, A.Y., 1992. Sediment facies, depositional environments, and distribution of phytoclasts in the recent Mahakam River delta, Kalimantan, Indonesia. Palaios 7, 574–590.

Gastaldo, R.A., Allen, G.P., Huc, A.Y., 1995. The tidal character of fluvial sediments of the modern Mahakam River delta, Kalimantan, Indonesia. In: Flemming, B.W., Bartholoma, A. (Eds.), Tidal Signatures in Modern and Ancient Sediments, Special Publication International Association of Sedimentologists, vol. 24, pp. 171–183.

Goodbred, Jr. S.L., Kuehl, S.A., 1999. Holocene and modern sediment budgets for the Ganges–Brahmaputra river system: evidence for highstand dispersal to flood-plain, shelf and deep-sea depocenters. Geology 27, 559–562.

Hanebuth, T.J.J., Stattegger, K., 2004. Depositional sequences on a late Pleistocene–Holocene tropical siliciclastic shelf (Sunda Shelf, southeast Asia). Journal of Asian Earth Sciences 23, 113–126.

Harris, P.T., Hughes, M.G., Baker, E.K., Dalrymple, R.W., Keene, J.B., 2004. Sediment transport in distributary channels and its export to the pro-deltaic environment in a tidally dominated delta: Fly River, Papua New Guinea. Continental Shelf Research 24, 2431–2454.

Hori, K., Saito, Y., Zhao, Q., Wang, P., 2002. Architecture and evolution of the tide-dominated Changjiang (Yangtze) River delta, China. Sedimentary Geology 146, 249–264.

Hori, K., Tanabe, S., Saito, Y., Haruyama, S., Nguyen, V., Kitamura, A., 2004. Delta initiation and Holocene sea-level change: example from the Song Hong (Red River) delta, Vietnam. Sedimentary Geology 164, 237–249.

Howes, J.V.C., 1997. Petroleum resources and petroleum systems of SE Asia, Australasia, Papua New Guinea and New Zealand. Proceedings Indonesian Petroleum Association, pp. 81–100.

Jones, B.G., Woodroffe, C.D., Martin, G.R., 2003. Deltas in the Gulf of Carpentaria, Australia; forms, processes, and products. In: Sidi, F.H., Nummedal, D., Imbert, P., Darman, H., Posamentier, H.W. (Eds.), Tropical Deltas of Southeast Asia; Sedimentology, Stratigraphy, and Petroleum Geology, SEPM Special Publication, vol. 76, pp. 21–43.

Konert, M., Vandenberghe, J., 1997. Comparison of laser grain size analysis with pipette and sieve analysis; a solution for the underestimation of the clay fraction. Sedimentology 44, 525–535.

Kuehl, S.A., Levy, B.M., Moore, W.S., Allison, M.A., 1997. Subaqueous of the Ganges–Brahmaputra river system. Marine Geology 144, 81–96.

Lambert, B., 2003. Micropaleontological Investigations in the Modern Mahakam Delta, East Kalimantan (Indonesia) 2003. Notebooks on Geology A02, Maintenon, France. http://paleopolis.rediris.es/cg/CG2003_A02_BL/.

Lesueur, P., Lesourd, S., Lefebvre, D., Garnaud, S., Brun Cottan, J.C., 2003. Holocene and modern sediments in the Seine Estuary (France); a synthesis. Journal of Quaternary Science 18, 339–349.

Magnier, P., Oki, T., Witoerlar Kartaadiputra, L., 1975. The Mahakam delta, Kalimantan, Indonesia. Proceedings 9th World Petroleum Congress, Tokyo, pp. 239–250.

Mahboob-ul-Kabir, M., Azam, M.H., Saha, B.C., Hye, J.M.A., 2002. Past studies and further scopes on wave modelling in the coastal region of Bangladesh. First Asia-Pacific DHI Software Conference, Bangkok, 2002. http://www.dhisoftware.com/Bangkok2002/Proceedings/Tracks/Marine_Track.htm.

Michels, K.H., Kudrass, H.R., Hübscher, C., Suckow, A., Wiedicke, M., 1998. The submarine delta of the Ganges–Brahmaputra: cyclone-dominated sedimentation patterns. Marine Geology 149, 133–154.

Murray, S.P., Arief, D., 1988. Throughflow into the Indian Ocean through the Lombok Strait, January 1985–January 1986. Nature 333, 444–447.

Nittrouer, C.A., Kuehl, S.A., Sternberg, R.W., Figueiredo, A.G., Faria, L.E.C., 1995. An introduction to the geological significance

of sediment transport and accumulation on the Amazon continental shelf. Marine Geology 125, 177–192.

Nittrouer, C.A., Kuehl, S.A., Figueiredo, A.G., Allison, M.A., Sommerfield, C.K., Rine, J.M., Faria, E.C., Silveira, O.M., 1996. The geological record preserved by Amazon shelf sedimentation. Continental Shelf Research 16, 817–841.

Payenberg, T.H.D., Sidi, H.F., Lang, S.C., 2003. Paleocurrents and reservoir orientation of Middle Miocene channel deposits in Mutiara field, Kutei Basin, East Kalimantan. In: Sidi, F.H., Nummedal, D., Imbert, P., Darman, H., Posamentier, H.W. (Eds.), Tropical Deltas of Southeast Asia; Sedimentology, Stratigraphy, and Petroleum Geology, SEPM Special Publication, vol. 76, pp. 255–266.

Roberts, H.H., Sydow, J., 1996. The offshore Mahakam delta: stratigraphic response of late Pleistocene-to-modern sea level cycle. Proceedings Indonesian Petroleum Association, vol. 25, pp. 147–161.

Roberts, H.H., Sydow, J., 2003. Late Quaternary stratigraphy and sedimentology of the offshore Mahakam delta, East Kalimantan (Indonesia). In: Sidi, F.H., Nummedal, D., Imbert, P., Darman, H., Posamentier, H.W. (Eds.), Tropical Deltas of Southeast Asia; Sedimentology, Stratigraphy, and Petroleum Geology, SEPM Special Publication, vol. 76, pp. 125–145.

Snedden, J.W., Sarg, J.F., Clutson, M.J., Maas, M., Okon, T.E., Carter, M.H., Smith, B.S., Kolich, T.H., Yazid Manson, M., 1996. Using sequence stratigraphic methods in high-sediment supply deltas: examples from the ancient Mahakam and Rajang–Lupar deltas. Proceedings Indonesian Petroleum Association, vol. 25, pp. 281–295.

Sternberg, R.W., Cacchione, D.A., Paulson, B., Kineke, G.C., Drake, D.E., 1996. Observations of sediment transport on the Amazon subaqueous delta. Continental Shelf Research 16, 697–715.

Suiter, S.S., 1996. Shallow 3-D seismic analysis of late Pleistocene lowstand deltas (Mahakam, Indonesia). Proceedings Indonesian Petroleum Association, vol. 25, pp. 347–351.

Swenson, J.B., Paola, C., Pratson, L., Voller, V.R., Murray, A.B., 2005. Fluvial and marine controls on combined subaerial and subaqueous delta progradation: morphodynamic modeling of compound-clinoform development. Journal of Geophysical Research 110, F02013. doi:10.1029/2004JF000265.

Syvitski, J.P.M., Peckham, S.D., Hilberman, R., Mulder, T., 2003. Predicting the terrestrial flux of sediment to the global ocean: a planetary perspective. Sedimentary Geology 162, 5–24.

Tanabe, S., Hori, K., Saito, Y., Hauyama, S., Vu, V.P., Kitamura, A., 2003. Song Hong (Red River) delta evolution related to millenium-scale Holocene sea-level changes. Quaternary Science Reviews 22, 2345–2361.

Tanean, H., Paterson, D.W., Endharto, M., 1996. Source provenance interpretation of Kutei Basin sandstones and the implications for tectono-stratigraphic evolution of Kalimantan. Proceedings Indonesian Petroleum Association, vol. 25, pp. 333–345.

Trevena, A.S., Partono, Y.J., Clarck, T., 2003. Reservoir heterogeneity of Miocene–Pliocene deltaic sandstones at Attaka and Serang field, Kutei basin, offshore East Kalimantan, Indonesia. In: Sidi, F.H., Nummedal, D., Imbert, P., Darman, H., Posamentier, H.W. (Eds.), Tropical Deltas of Southeast Asia; Sedimentology, Stratigraphy, and Petroleum Geology, SEPM Special Publication, vol. 76, pp. 235–254.

Visser, M.J., 1980. Neap–spring cycles reflected in Holocene subtidal large-scale bedform deposits: a preliminary note. Geology 8, 543–546.

Wilson, M.E.J., Lokier, S.W., 2002. Siliciclastic and volcaniclastic influences on equatorial carbonates: insights from the Neogene of Indonesia. Sedimentology 49, 583–601.